Enhancement of Breakdown Voltage in AlGaN/GaN High Electron Mobility Transistors Using Double Buried p-Type Layers *

Jun Luo(罗俊)[1], Sheng-Lei Zhao(赵胜雷)[1], Zhi-Yu Lin(林志宇)[1], Jin-Cheng Zhang(张进成)[1], Xiao-Hua Ma(马晓华)[1,2], Yue Hao(郝跃)[1]**

[1]*Key Laboratory of Wide Band-Gap Semiconductor Materials and Devices, School of Microelectronics, Xidian University, Xi'an 710071*

[2]*School of Advanced Materials and Nanotechnology, Xidian University, Xi'an 710071*

(Received 10 January 2016)

A novel AlGaN/GaN high electron mobility transistor (HEMT) with double buried p-type layers (DBPLs) in the GaN buffer layer and its mechanism are studied. The DBPL AlGaN/GaN HEMT is characterized by two equi-long p-type GaN layers which are buried in the GaN buffer layer under the source side. Under the condition of high-voltage blocking state, two reverse p–n junctions introduced by the buried p-type layers will effectively modulate the surface and bulk electric fields. Meanwhile, the buffer leakage is well suppressed in this structure and both lead to a high breakdown voltage. The simulations show that the breakdown voltage of the DBPL structure can reach above 2000 V from 467 V of the conventional structure with the same gate–drain length of 8 μm.

PACS: 73.40.Kp, 73.61.Ey, 78.30.Fs DOI: 10.1088/0256-307X/33/6/067301

In recent years, AlGaN/GaN high-electron mobility transistors (HEMTs) have been widely investigated as promising candidates for power electronics applications due to their superior properties, such as high critical breakdown electric field, high saturation velocity and high two-dimensional electron gas (2DEG) density.[1–4] There still exists a huge gap between the actual breakdown voltages (BVs) and the theoretical values for AlGaN/GaN HEMT power devices, indicating that the breakdown voltage can be further improved.[5,6] The breakdown in AlGaN/GaN HEMTs is due to an avalanche process triggered by the impact ionization that is usually caused by the electric field crowding at the drain-side edge of the gate and the buffer leakage current has significant impact on avalanche process. Thus breakdown can be improved by relieving the peak electric field at the drain-side edge of the gate and/or by decreasing the buffer leakage.

So far, efforts to spread the electric field and to increase BV in AlGaN/GaN HEMTs have utilized both/either a larger gate to drain separation ($L_{\rm dg}$) and/or the extension of the gate as a field plate (FP) over an insulator deposited in the gate to drain separation.[5,7,8] For the former technique, the BV-$L_{\rm gd}$ dependences were reported in the past saturation at large $L_{\rm gd}$, limiting the achievable BV values to 400–600 V. For the latter technique, even after careful optimization of the FP geometry, significant further increase is possible only by strongly varying the insulator thickness (by a factor of 5 or more) along the FP length[8] or using multiple field plates design,[9] obtained BV beyond 1000 and 900 V correspondingly. However, processing such a variable thickness insulator of controlled dimension or multiple metal layers may be difficult.

To achieve higher BV in AlGaN/GaN HEMTs, it is necessary to make the leakage through the underlying GaN buffer as low as possible. Techniques like incorporating Fe-doping in metal-organic chemical vapor deposition (MOCVD) grown GaN buffers[10] and C-doping in molecular beam epitaxy (MBE) grown GaN buffers[11,12] are commonly used to reduce the buffer leakage.[13–15] However, subsequently introduced impurity scattering may deteriorate the other performances of HEMTs.

In this Letter, a novel AlGaN/GaN HEMT with double buried p-type layers (DBPLs) in the GaN buffer layer is proposed, which utilizes the effect of bulk electric field modulation to increase the BV being similar to the reduced bulk field (REBULF)[16–18] in silicon power devices. The device structures and characteristics of the DBPL AlGaN/GaN HEMT have been simulated with a Sentaurus TCAD software. The surface and bulk electric fields in the AlGaN/GaN HEMT are optimized effectively by the DBPL, and the electrons in the buffer are fully depleted in this structure, both leading to a significant improvement of BV. By introducing the DBPL into the unintentionally doped n-GaN buffer layer, the surface and bulk electric fields of the device are redistributed and the uniformity of electric field is improved by utilizing the reverse-biased DBPL/n-GaN buffer junctions, meanwhile the buffer leakage is well suppressed in this structure and the obtained BV is beyond 2000 V.

The DBPLs and the conventional AlGaN/GaN HEMTs are shown in Fig. 1. Compared with the conventional structure, two equi-long p-type GaN layers are buried in the GaN buffer layer on the source side. Here L represents the length of the buried p-

*Supported by the National Natural Science Foundation of China under Grant Nos 61334002, 61106106, and 61204085, and the China Postdoctoral Science Foundation Funded Project under Grant No 2015M582610.

**Corresponding author. Email: yhao@xidian.edu.cn

© 2016 Chinese Physical Society and IOP Publishing Ltd

type layer, T_1 is the distance of two p-layers, which is equal to the distance of the first p-layer and the AlGaN layer, and T_2 is the thickness of the buried p-type layer.

The double p-type layers are buried in the proposed structure to obtain an enhanced modulation effect for the bulk electric field in comparison with only one p-type layer. When a high positive voltage V_d is applied to the drain on the off-state of the DBPL AlGaN/GaN HEMT, two reverse p–n junctions introduced by the buried p-type layers will lead to a new electric field peak at the position, which will effectively modulate the surface and bulk electric fields and will result in a higher BV for the DBPL device.

Two-dimensional device simulations for the proposed DBPL AlGaN/GaN HEMT specified in Table 1 are performed to verify the device operation. To simplify the simulation process, T_2 is set to be equal to T_1 in this work. The BV is the off-state I_{ds}–V_{ds} curve with $V_{gs} = -6$ V, which is defined as the drain voltage for the drain current of 1 mA/mm.

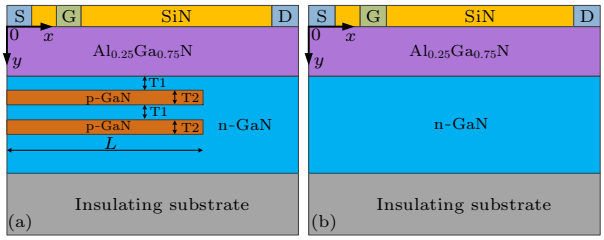

Fig. 1. (Color online) Schematic structures of (a) the DBPL AlGaN/GaN HEMT and (b) the conventional AlGaN/GaN HEMT.

Table 1. Device parameters used in the simulation.

Device parameters	DBPL HEMT	Con. HEMT
Length of source, L_s	1 μm	1 μm
Length of source-gate spacing, L_{gs}	1 μm	1 μm
Length of gate, L_g	1 μm	1 μm
Length of drain-gate spacing, L_{gd}	8 μm	8 μm
Length of drain, L_d	1 μm	1 μm
Thickness of AlGaN layer, t_{AlGaN}	0.03 μm	0.03 μm
Thickness of GaN buffer layer, t_{GaN}	3 μm	3 μm
Length of the buried p-type layer, L	6–9 μm	0 μm
Distance of two p-layers, T_1	0.1–0.3 μm	0 μm
Thickness of the buried p-type layers, T_2	0.1–0.3 μm	0 μm
Sheet carrier density, n_s	6×10^{12} cm^{-2}	6×10^{12} cm^{-2}
Concentration of AlGaN barrier layer, N_{AlGaN}	1×10^{15} cm^{-3}	1×10^{15}cm^{-3}
Concentration of GaN buffer layer, N_{GaN}	1×10^{15} cm^{-3}	1×10^{15}cm^{-3}
Concentration of the buried p-type layers, N_{BP}	optimized	0 cm^{-3}

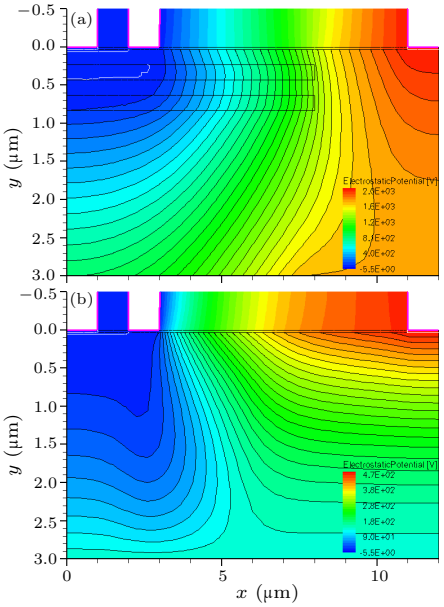

Fig. 2. (Color online) Equipotential contour distributions at breakdown for (a) the DBPL AlGaN/GaN HEMT and (b) for the conventional AlGaN/GaN HEMT. Here $T_1 = T_2 = 0.2$ μm and $L = 8$ μm for the DBPL structure.

Figure 2 shows the equipotential contour distributions at breakdown for the DBPL AlGaN/GaN HEMT and the conventional AlGaN/GaN HEMT. For the DBPL structure, $T_1 = T_2 = 0.2$ μm and $L = 8$ μm. It can be clearly seen that due to the modulating effect of the double buried p-type layers, the equipotential contour distributions of the DBPL structure are more uniform than those of the conventional structure, especially at the edge of the buried p-type layer, which contributes to a higher BV for the DBPL structure.

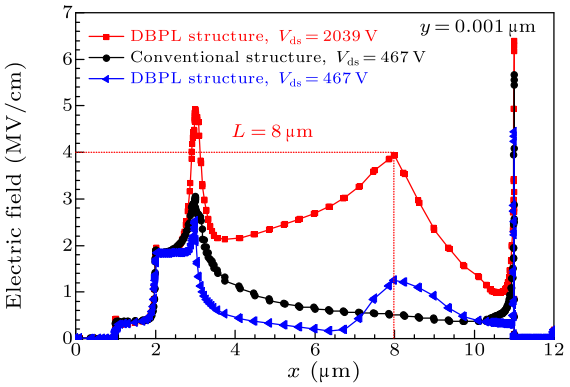

Fig. 3. (Color online) Distributions of surface electric field at breakdown for the DBPL AlGaN/GaN HEMT and for the conventional AlGaN/GaN HEMT. Here $T_1 = T_2 = 0.2$ μm and $L = 8$ μm for the DBPL structure.

Figure 3 is the distributions of surface electric fields ($y = 0.001$ μm) at breakdown for the DBPL AlGaN/GaN HEMT and the conventional AlGaN/GaN HEMT. Due to the introduced reverse p–n junction

by the buried p-GaN layer, a new surface electric field peak is produced for the DBPL structure, which means that the lateral electric field of the DBPL structure is effectively optimized. It can be obviously seen that the peak of lateral electric field for the DBPL AlGaN/GaN HEMT is lower than that for the conventional AlGaN/GaN HEMT at the same bias $V_{ds} = 467$ V. Figure 4 shows the electron concentration distribution of the AlGaN/GaN HEMTs with $V_{gs} = -6$ V and $V_{ds} = 400$ V, and the white line is the boundary of the depletion region. It can be seen that the p-GaN buried layers have not been completely depleted under the bias condition $V_{ds} = 400$ V. For the DBPL structure, the electrons in the buffer are fully depleted, effectively suppressing the buffer leakage current. Therefore, the DBPL structure can alleviate the buffer-leakage-induced impact ionization which may initiate the avalanche process compared with the conventional structure, and the suppression of the impact ionization is the other reason for the enhancement of BV.[1,13,14]

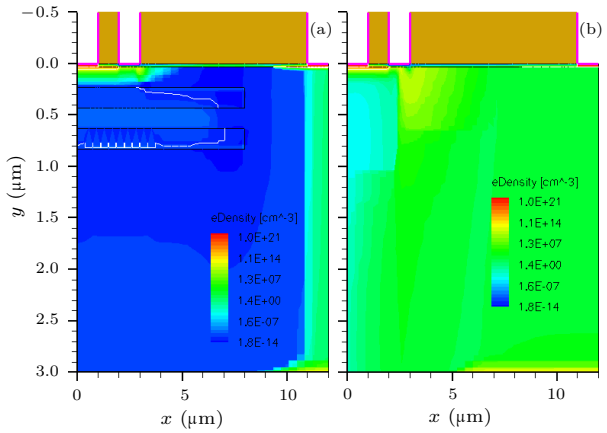

Fig. 4. (Color online) Off-state electron concentration distributions of (a) the DBPL AlGaN/GaN HEMT and (b) the conventional AlGaN/GaN HEMT. Both the devices are biased at $V_{gs} = -6$ V and $V_{ds} = 400$ V.

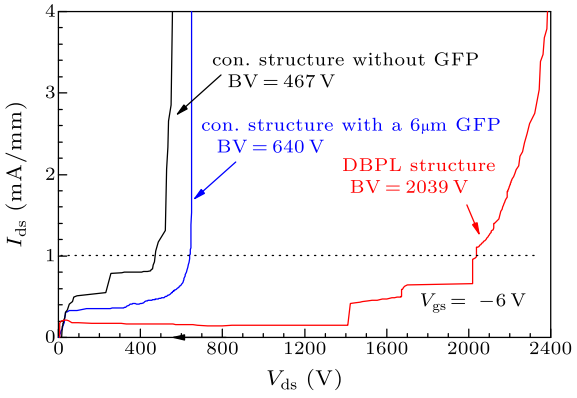

Fig. 5. (Color online) Off-state I–V characteristics of the DBPL AlGaN/GaN HEMT, the conventional AlGaN/GaN HEMT without the GFP and the conventional AlGaN/GaN HEMT with a 6 μm GFP. Here $T_1 = T_2 = 0.2$ μm, $L = 8$ μm for the DBPL structure, and the thickness of SiN beneath the GFP is 0.3 μm.

The conventional-structure AlGaN/GaN HEMT with a gate field plate (GFP) is also simulated herein for comparison. Figure 5 shows the off-state I–V characteristics for these devices. The BV of the proposed DBPL structure is increased to 2039 V from the 467 V of the conventional structure without the GFP, and the BV of the conventional structure with a 6 μm GFP is 640 V. It can be seen that the DBPL structure has a much higher BV than the GFP structure AlGaN/GaN HEMT.

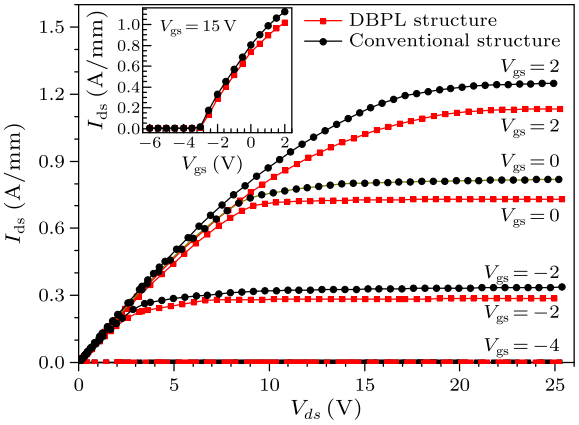

Fig. 6. (Color online) On-state I–V characteristics and transfer characteristics of the DBPL AlGaN/GaN HEMT and the conventional AlGaN/GaN HEMT. Here $T_1 = T_2 = 0.2$ μm and $L = 8$ μm for the DBPL structure.

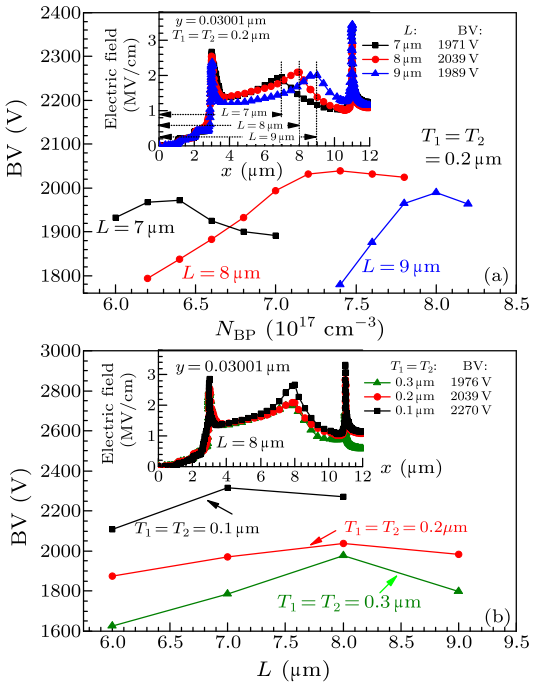

Fig. 7. (Color online) Influences of device parameters on breakdown characteristics: (a) N_{BP} and L on the BV, and interface electric field distributions at the BV with different L, and (b) L and T_1/T_2 on the BV, and interface electric field distributions at the BV with different T_1/T_2.

Figure 6 shows the on-state I–V characteristics of the DBPL AlGaN/GaN HEMT and the conventional AlGaN/GaN HEMT, the inset presents their transfer characteristics. It can be seen that the on-

state resistance R_{on} of the DBPL AlGaN/GaN HEMT is slightly larger than the conventional AlGaN/GaN HEMT, while the magnitude of the BV increase is even greater for the DBPL AlGaN/GaN HEMT, and leads to a higher figure of merit (FOM).

Figure 7 shows the influences of structure parameters on breakdown characteristics for the DBPL AlGaN/GaN HEMT. Figure 7(a) shows the influences of N_{BP} and L on the BV with $T_1 = T_2 = 0.2\,\mu m$, the inset is the interface electric field distributions at the BV with different L. It can be seen that there is an optimized N_{BP} to reach the highest BV for each L, and the optimized N_{BP} increases with L rising from 7 to 9 μm. The largest BV of 2039 V is obtained when $L = 8\,\mu m$ and $N_{BP} = 7.4 \times 10^{17}\,cm^{-3}$ for the DBPL AlGaN/GaN HEMT due to its best electric field modulation effect on the interface of AlGaN/GaN. Figure 7(b) shows the influences of L and T_1/T_2 on BV, the inset is the interface electric field distributions at the BV with different T_1/T_2. The BV is enhanced with the decrease of T_1/T_2. When $T_1 = T_2 = 0.1\,\mu m$, the BV of the DBPL AlGaN/GaN HEMT can reach 2316 V. It can be seen that the introduced new electric field peak is more obvious when the thicknesses of buried p-type layers are thinner. This is due to the fact that the optimized N_{BP} is higher when the thicknesses of buried p-type layers are thinner, which leads to a larger difference between the concentration of p-type area and n-type area in the p–n junctions. It can be concluded that thinner double buried p-type layers should help achieve a more significant electric field modulation, and lead to a high BV.

In summary, an AlGaN/GaN HEMT with DBPLs in the GaN buffer has been proposed. It provides a new method to effectively increase the BV for the AlGaN/GaN HEMT. The DBPL AlGaN/GaN HEMT is potential for applications in high voltage and power areas due to its favorable performances.

References

[1] Zhao S L, Hou B, Chen W W, Mi M H, Zheng J X, Zhang J C, Ma X H and Hao Y 2016 *IEEE Trans. Power Electron.* **31** 1517
[2] Luo J, Zhao S L, Mi M H, Chen W W, Hou B, Zhang J C, Ma X H and Hao Y 2016 *Chin. Phys.* B **25** 027303
[3] Chu R M, Corrion A, Chen M, Li R, Wong D, Zehnder D, Hughes B and Boutros K 2011 *IEEE Electron Device Lett.* **32** 632
[4] Zhao S L, Chen W W, Yue T, Wang Y, Luo J, Mao W, Ma X H and Hao Y 2013 *Chin. Phys.* B **22** 117307
[5] Karmalkar S and Mishra U K 2001 *IEEE Trans. Electron Devices* **48** 1515
[6] Karmalkar S, Deng J Y, Shur M S and Gaska R 2001 *IEEE Electron Device Lett.* **22** 373
[7] Tipirneni N, Koudymov A, Adivarahan V, Yang J, Simin G and Khan M A 2006 *IEEE Electron Device Lett.* **27** 716
[8] Karmalkar S and Mishra U K 2001 *Solid-State Electron.* **45** 1645
[9] Xing H L, Dora Y, Chini A, Heikman S, Keller S and Mishra U K 2004 *IEEE Electron Device Lett.* **25** 161
[10] Heikman S, Keller S, DenBaars S P and Mishra U K 2002 *Appl. Phys. Lett.* **81** 439
[11] Poblenz C, Waltereit P, Rajan S, Heikman S, Mishra U K and Speck J S 2004 *J. Vac. Sci. Technol.* B **22** 1145
[12] Bahat-Treidel E, Brunner F, Hilt O, Cho E, Würfl J and Tränkle G 2010 *IEEE Trans. Electron Devices* **57** 3050
[13] Dora Y, Chakraborty A, Heikman S, McCarthy L, Keller S, DenBaars S P and Mishra U K 2006 *IEEE Electron Device Lett.* **27** 529
[14] Verzellesi G, Morassi L, Meneghesso G, Meneghini M, Zanoni E, Pozzovivo G, Lavanga S, Detzel T, Häberlen O and Curatola G 2014 *IEEE Electron Device Lett.* **35** 443
[15] Uren M J, Silvestri M, Cäsar M, Hurkx G A M, Croon J A, Šonský J and Kuball M 2014 *IEEE Electron Device Lett.* **35** 327
[16] Cheng J B, Zhang B, Sun W F, Shi L X and Li Z J 2014 *Superlattices Microstruct.* **76** 288
[17] Cheng J B, Zhang B and Li Z J 2008 *Electron. Lett.* **44** 933
[18] Zhang B, Duan B X and Li Z J 2006 *Chin. J. Semicond.* **27** 730